Analysis of Crop Spectral Reflectance at the Croplands in Eastern Kazakhstan Using Satellite Imagery

Samarkhanov, K.,[1,2] Sadenova, M.[1*] and Beisekenov, N.,[1]
[1]Veritas Center of Excellence, D. Serikbayev East Kazakhstan Technical University, Kazakhstan
E-mail: msaden- ova@edu.ektu.kz
[2]Kazakhstan Gharysh Sapary National Company JSC, Kazakhstan, E-mail: k.samarkhanov@gharysh.kz
Corresponding Author

DOI: https://doi.org/10.52939/ijg.v19i11.2923

Abstract

Using satellite imagery, this study investigates the spectral reflectance characteristics of crops at the OHMK farm in Eastern Kazakhstan, focusing on wheat and barley. The analysis reveals significant differences in spectral re- flectance, particularly in the visible and near-infrared regions, and tracks change over time during different growth stages. Employing principal component analysis (PCA), strong correlations are observed between specific spectral bands and principal components, providing insights into crop variability. Derived equations enable the estimation of principal component values based on spectral information. These findings have implications for crop monitoring, management, and precision agriculture, offering potential yield optimization and resource allocation improvements. The study highlights the potential use of spectral reflectance analysis for crop health assessment and yield prediction, with implications for agricultural decision-making and enhanced productivity. Further research is needed to expand the application of this approach to other crops and conditions.

Keywords: Deformation, Earthquake, GNSS, Risk Zone, Velocities

1. Introduction

Remote sensing technology, especially satellite imagery, has revolutionized monitoring, managing, and predicting crop performance, leading to a more sustainable and productive agricultural sector. A vital component of this techno-logical revolution is the study of crop reflectance, a non-invasive and highly informative method to assess crop health and predict yields [1] and [2]. Crop reflectance refers to how crops absorb, transmit, and reflect light across different wavelengths. By analyzing the light reflected from crops, scientists can infer valuable information about the plant’s health, growth stage, and productivity. This light can range from the visible spectrum to near and far infrared, with different crops and conditions altering the specific reflectance patterns [3] and [4].

In the visible light range, healthy vegetation typically absorbs most blue and red light due to chlorophyll, essential for photosynthesis. This light absorption causes healthy plants to reflect more green light, making them appear green to the human eye. On the other hand, in the near-infrared region, healthy plants reflect a lot of light, a characteristic known as the ’red edge.’ This high reflectance is due to the plant’s cellular structure, which scatters light in the near- infrared [5]. The Normalized Difference Vegetation Index (NDVI) is a popular measure used in remote sensing. It captures the difference between near-infrared (which vegetation strongly reflects) and red light (which vegetation absorbs) to assess plant health and vigor [6]. Tasseled Cap Transformation (TCT) is another technique developed explicitly for Landsat data, yielding three components- brightness, greenness, and wetness-representing soil brightness, vegetation cover, and moisture content, respectively [7].

In remote sensing, PCA is often used for data reduction when dealing with multi-band images. It is a statistical procedure that transforms a set of observations of possibly correlated variables into values of linearly uncorrelated variables called principal components [8]. Each principal component explains a certain percentage of the total variation in the dataset, with the first few components typically explaining the majority of the variation. PCA can help reduce the complexity of multi-dimensional data, making it easier to interpret spectral reflectance patterns across different crops and growth stages [9].

Remote sensing data can also be used to predict crop yields. By correlating historical yield data with spectral characteristics of the crops at different growth stages, machine learning algorithms can be trained to predict future yields based on remote sensing data [10]. Time-series analysis of remote sensing data can monitor the phenological stages of crops, providing crucial information about the timing of key growth stages, such as flowering or maturity [11].

By measuring and analyzing these reflectance patterns, remote sensing applications can detect subtle changes in plant health long before they become visible to the human eye [12]. For instance, a stressed plant might reflect more light in the visible spectrum and less in the near-infrared, indicating potential issues such as disease, nutrient deficiency, or drought stress [13]. This capability to 'see' the unseeable makes crop reflectance studies using remote sensing a powerful tool in modern agriculture. By enabling early detection of plant stress, it allows for timely intervention, ultimately leading to better crop management and improved yields [14]. Furthermore, farmers and policymakers can make informed decisions about crop marketing and food supply logistics by predicting crop yields based on reflectance data, contributing to a more efficient and sustainable agricultural system.

Combined with data processing and machine learning advances, these methods hold significant potential for enhancing crop management and increasing agricultural productivity [15]. While this technology holds immense promise, it is essential to consider local crop types, growth stages, and environ- mental conditions when interpreting reflectance data. As such, studies like the one on wheat and barley at the OHMK farm in Eastern Kazakhstan are crucial in expanding our understanding of spectral reflectance across different crops and environments.

2. Methods

The research area is located in the Eastern Kazakhstan province north of Ust-Kamenogorsk city and is a farmland area with various crops (Figure 1). The relief of the study area refers to the variations in elevation across the landscape. The statistical analysis reveals essential characteristics of the relief. The maximum elevation of 612 meters indicates the highest point in the area, while the minimum elevation of 296 meters represents the lowest point. The mean elevation of 400.1 meters provides an average value, representing the typical height of the terrain. The standard deviation of 45.5 meters indicates the degree of variation or spread of the elevation values around the mean. We created the dataset using the Google Earth Engine web service [16]. It included elevation [17], soil bulk density [18], rainfall data [19], spectral reflectance data captured by Landsat-8 [20] on 21.06.2022, 08.08.2022, 24.08.2022, also Land use data with exact crop species information collected on August 9th, 23rd, and October 20th, 2022 by our group under this Research grant (Table 1). This table provides an overview of the input dataset details used in the study. It includes information on the type of data, the product/source name, and specific details such as spatial resolution and layers.

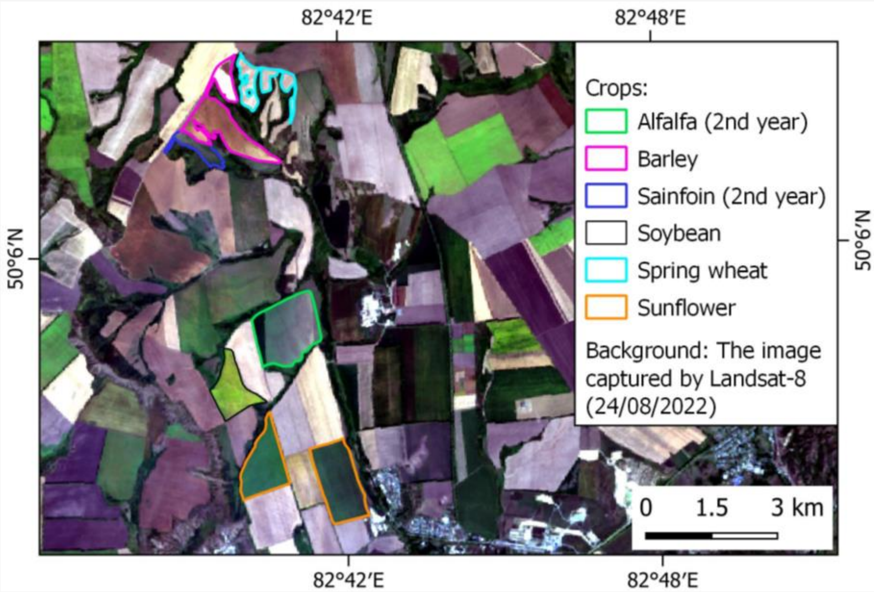

Figure 1: The study area

Table 1: Input dataset details

No.	Data	Product	Details
1	Elevation	NASADEM$_{HGT}$ v001	Spat. Res. 30 m
2	Spectral reflectance	LANDSAT-8 (CO2, T1$_{L2}$)	Spat. Res. 30 m (R, G, B, NIR, SWIR1-2)
3	Soil bulk density	OpenLandMap, v02	0-30 cm layer, Spat. Res. 250 m
4	Rainfall data	OpenLandMap, v01	Spat. Res. 250 m
5	Field data	Land use information	Under Research Grant in 2022

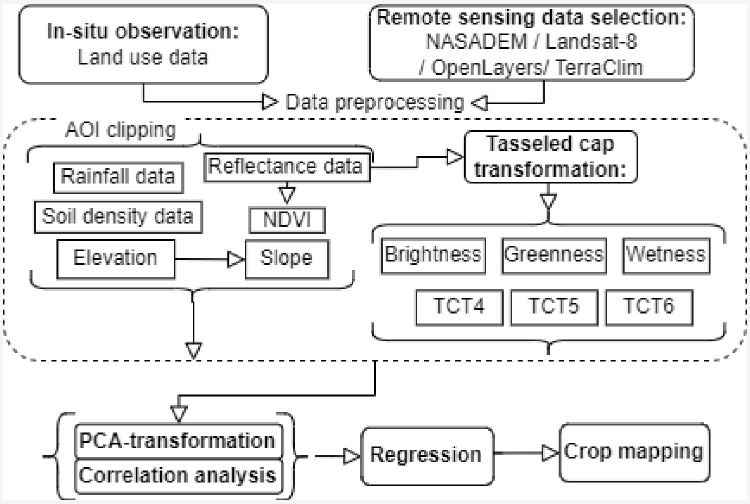

Figure 2: The research design

Table 2: The tasseled cap transformation coefficients for Landsat-8 [21]

Blue	Green	Red	NIR	SWIR1	SWIR2
0.3029	0.2786	0.4733	0.5599	0.508	0.1872
-0.2941	-0.243	-0.5424	0.7276	0.0713	-0.1608
0.1511	0.1973	0.3283	0.3407	-0.7117	-0.4559
-0.8239	0.0849	0.4396	-0.058	0.2013	-0.2773
-0.3294	0.0557	0.1056	0.1855	-0.4349	0.8085
0.1079	-0.9023	0.4119	0.0575	-0.0259	0.0252

The research workflow included data collection and preprocessing (the data clipping, NDVI calculation, and the Tasseled Cap Transformation), the PCA transformation, the data correlation, and the crop mapping (Figure 2). Tasseled Cap Transformation (TCT) and Principal Component Analysis (PCA) are widely used remote sensing techniques for image interpretation and data reduction. Tasseled Cap Transformation is a linear transformation developed for Landsat satellite data (Table 2). The transformation involves converting the original satellite bands into new components that are easier to interpret regarding physical vegetation characteristics. The three primary TCT components are brightness, greenness, and wet- ness, representing soil brightness, vegetation cover, and moisture content. In the context of crop reflectance, TCT can provide valuable insights into the crop's health and growth stages. Principal Component Analysis (PCA) was applied [22], and it consisted of the following steps:

1. The dataset was standardized.
2. The covariance matrix C of the data was computed using equation 1.

$$C = \frac{1}{n-1} X^T X$$

Equation 1

where X is the data matrix, X^T represents the transpose of matrix X, and n is the number of data points.

3. The eigenvalues and eigenvectors of the covariance matrix were computed.
4. The eigenvalues and corresponding eigenvectors in decreasing order were sorted.

After the Tasseled cap transformation, correlation (Pearson's coefficient) and statistical significance (p-values) for all data were tested. In the context of the study on wheat and barley at the OHMK farm in Eastern Kazakhstan, TCT and PCA are valuable tools. TCT helps interpret the spectral reflectance data regarding physical crop characteristics. At the same time, PCA simplifies the multi-dimensional reflectance data, making it easier to identify key patterns and differences between the crops. At the final stage, multiple linear regression equations were formulated to map the selected crops in the study area.

3. Results and Discussion

The p-values for each crop and parameter combination indicate the statistical significance of the difference between the sample mean and the null hypothesis mean (zero). A p-value less than the significance level (e.g., 0.05) indicates that the difference is statistically significant. Based on the provided p-values, here are some conclusions:

For Spring wheat, most parameters (*Red*, *Green*, *Blue*, *NIR*, *SWIR1*, *SWIR2*, Brightness, *Greenness*, *TCT4*, *TCT5*, *TCT6*, *NDVI*, *PC1*, and *PC2*) have extremely low p-values close to zero, indicating a significant difference from the null hypothesis mean of zero. Wetness also has a very low p-value, suggesting a significant difference.

For Barley, like Spring wheat, most parameters have extremely low p-values close to zero, indicating a significant difference from the null hypothesis mean of zero. For Sainfoin, most parameters have very low p-values close to zero, indicating a significant difference. *PC1* has a higher p-value (1.34), suggesting less statistical significance than other parameters.

For Alfalfa (2nd year), most parameters have p-values equal to zero, indicating a significant difference from the null hypothesis mean of zero. *PC1* has a higher p-value (0.85), suggesting less statistical significance than other parameters. For Sunflower and Soybean, like Spring wheat and Barley, most parameters have extremely low p-values close to zero, indicating a significant difference from the null hypothesis mean of zero.

These results suggest that for most parameters, there is a significant difference in the mean values between the crops, indicating potential discriminative power in distinguishing the crops based on those parameters.

However, interpreting the results should consider other factors, such as the data distribution, sample size, and specific research objectives. Due to a low statistical significance, results do not include elevation, Slope, Soil density, and Rainfall data.

After that, Pearson's correlation tests were applied to the research dataset, and the results demonstrated specific strong values according to the Table 3. Observed correlations between *PC1*, *PC2*, and the listed parameters for each crop demonstrated positive and negative values described below:

a) Spring wheat [23]: *PC1* shows high positive correlations with *Greenness* data (*TCT*), *Green*, *Blue*, and *SWIR2* bands, while it has a strong negative correlation with *NDVI* and *TCT4*. *PC2* has no significant correlations.
b) Barley [24]: *PC1* exhibits significant positive correlations with *Red*, *Green*, and *SWIR2* bands and strong negative with *NDVI*. *PC2* shows negative correlations with *SWIR1* and *SWIR2*.
c) Sainfoin [25] : *PC1* positively correlates with *Greenness* data, *Green*, *SWIR2*, *Red* bands, and *NDVI*. *PC2* shows negative correlations with the *Red*, *SWIR1*, and *SWIR2* bands.
d) Alfalfa [26] (2nd year): *PC1* is positively correlated with *TCT6* and negatively with *SWIR2*. *PC2* positively correlates with *NIR*, *Greenness* and has a moderate correlation with *NDVI*.
e) Sunflower [27]: *PC1* exhibits positive correlations with *SWIR1*, *SWIR2*, and *NIR*, strongly correlates negatively with *NDVI*. *PC2* positively correlates with *SWIR2*, *SWIR1*, and *NIR* and has a moderate negative correlation with *NDVI*.
f) Soybean [28]: *PC1* shows a negative correlation with *Greenness* data and *NDVI* and positive correlations with *SWIR1*, *SWIR1*, *NIR*, and *Red*. *PC2* does not show any significant correlations with the listed parameters.

These correlations provide insights into the relationships between the principal components (*PC1*, *PC2*) and the corresponding parameters for each crop. We plotted the strongest values to visualize some of the described correlations for crops (Figure 3). This figure demonstrates the negative correlation values of vegetation-related information (*NDVI*) for Barley, Sainfoin, Spring wheat, Soybean, and Sunflower. At the same time, Alfalfa showed high positive values between principal component 2 and *NIR* reflectance band.

Table 3: Correlation values for *PC1* and *PC2*

Crop	*PC1*	*PC2*
Spring wheat	Greenness (0.98), Green (0.9), Blue (0.89), SWIR2 (0.96), TCT4 (-0.97), NDVI (-0.98)	-
Barley	Red (0.9), Green (0.77), SWIR2 (0.8), NDVI (-0.92)	SWIR1 (-0.88), SWIR2 (-0.83)
Sainfoin	Greenness (0.87), Green (0.89), SWIR2 (0.87), Red (0.85), NDVI (-0.92)	SWIR1 (-0.91), SWIR2 (-0.91), Red (-0.79)
Alfalfa (2nd year)	TCT6 (0.89), SWIR2 (-0.96)	NIR (0.99), Greenness (0.98), NDVI (0.75)
Sunflower	SWIR1 (0.97), SWIR2 (0.98), NIR (0.93), NDVI (-0.97)	SWIR1 (0.88), SWIR2 (0.88), NIR (0.79), NDVI (-0.85)
Soybean	Greenness (-0.8), SWIR1 (0.92), SWIR2 (0.91), NIR (0.89), Red (0.92), NDVI (-0.97)	-

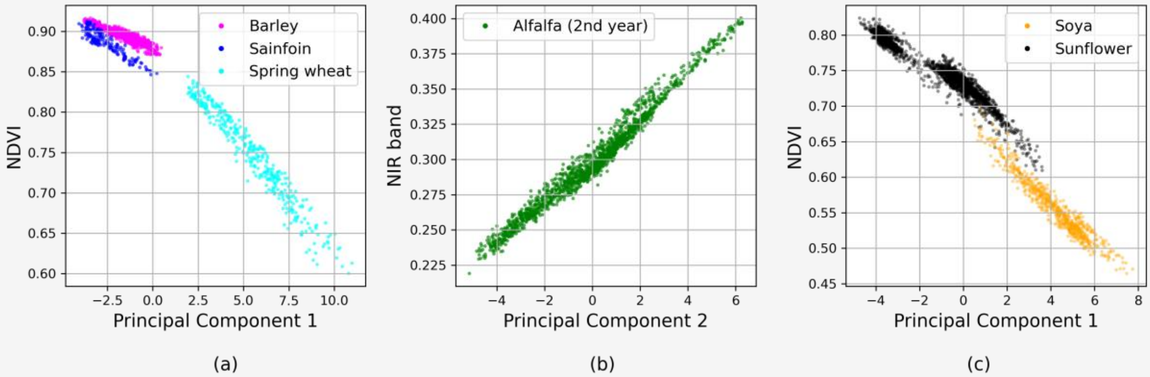

Figure 3: The correlation between principal components and vegetation-related data (a) barley sainfoin and spring wheat (b) alfalfa (c) soya and sunflower

The next step of this research included formulating multiple linear equations based on the observed correlations. Therefore, the principal components (*PC1*, *PC2*) are considered dependent parameters, while others are independent as illustrates in equations 2 to 5:

Spring wheat:

$$PC1 = 157.3Greeness - 15.4Blue + 10.6SWIR2 - 22.4Green - 9.7TCT\,4 - 10.9\,NDVI + 7.6$$

Equation 2

This regression equation represents the relationship between *PC1* and the Spring wheat crop's input features (*Greeness*, *Green*, *Blue*, *SWIR2*, *TCT4*, and *NDVI*). The coefficients indicate the magnitude and direction of the impact of each input feature on *PC1*.

Barley:

$$PC1 = -206.2Red + 177.73Green + 12.85WIR2 - 103.37NDVI + 86.12$$

Equation 3

This equation represents the relationship between *PC1* and the Barley crop's input features (*Red*, *Green*, *SWIR2*, and *NDVI*). The coefficients indicate how changes in each input feature influence *PC1*.

Sainfoin:

$$PC1 = 198.33Red + 62.31Green + 51.11SWIR2 - 39.33Greenness + 35.53NDVI - 32.64$$

Equation 4

This equation represents the relationship between *PC1* and the input features (*Red*, *Green*, *SWIR2*, *Greenness*, and *NDVI*) for the Sainfoin crop. The coefficients indicate the strength and direction of the influence of each input feature on *PC1*.

Alfalfa:

$$PC2 = 105.02NIR - 82.63Greenness + 19.48NDVI - 30.6$$

Equation 5

This equation represents the relationship between *PC2* and the Alfalfa crop's input features (*NIR*, *Greenness*, and *NDVI)*. The coefficients indicate the impact of each input feature on *PC2* are presented in equation 6 and 7.

Sunflower:

$$PC1 = -15.27NIR + 57.16SWIR1 - 11.87SWIR2 - 15.25NDVI + 7.0$$

Equation 6

This equation represents the relationship between *PC1* and the Sunflower crop's input features (*NIR*, *SWIR1*, *SWIR2*, and *NDVI*). The coefficients indicate the strength and direction of the influence of each input feature on *PC1*.

Soybean:

$$PC1 = 97.38\ Red - 17.74NIR + 12.24SWIR1 + 20.61SWIR2 + 2.24NDVI - 5.25$$

Equation 7

This equation represents the relationship between *PC1* and the input features (*Red*, *NIR*, *SWIR1*, *SWIR2*, and *NDVI*) for the Soybean crop. The coefficients indicate the impact of each input feature on *PC1*. These regression equations provide a mathematical representation of the relationship between the principal component *PC1* and the input features for each crop. Using the coefficients, we estimated the *PC1* and *PC2* based on the given input features using input raster data. We derived the principal components map that mainly exposes vegetation growth in the study area croplands (Figure 4). The description of the PCA values for each crop is provided in Table 4, which includes the maximum, mean, minimum, and standard deviation of the PCA values for each crop. It overviews the distribution and variation in PCA values across the crops. These values provide insights into each crop's distribution and variation of PCA values. The maximum PCA value represents the highest level of variability, while the mean PCA value indicates the average level of variability. The standard deviation shows the spread of PCA values around the mean. Comparing the crops, Sunflower exhibits the highest maximum PCA value, indicating more significant variability compared to other crops. At the same time, Barley shows the lowest mean and standard deviation, suggesting relatively lower variability.

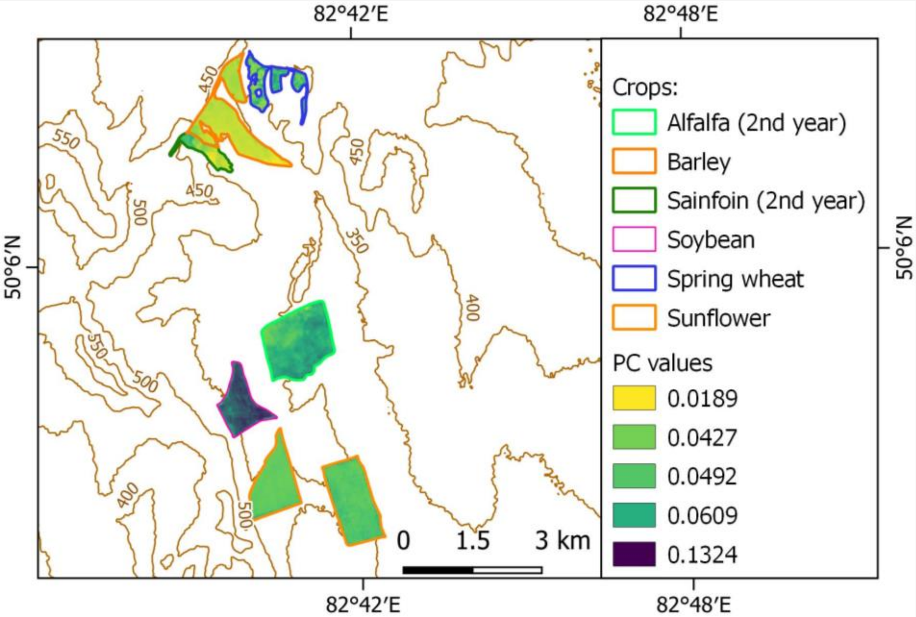

Figure 4: The map of the *PC* values distribution for crops in the study area

Table 4: PCA statistics for each crop

Crop	Maximum	Mean	Minimum	Standard Deviation
Spring wheat	0.0978	0.0152	0	0.0235
Barley	0.0564	0.0085	0	0.0139
Sainfoin	0.0733	0.0377	0	0.0125
Alfalfa	0.0886	0.0434	0	0.0283
Sunflower	0.1324	0.0181	0	0.0242
Soybean	0.1203	0.0398	0	0.0474

We can gain insights into spectral characteristics and variability by comparing these statistical measures across different crops. For example, crops with higher maximum and mean PCA values exhibit more significant spectral variability, indicating diverse and distinct spectral signatures. Conversely, crops with lower maximum and mean PCA values have less spectral variability and may exhibit more uniform spectral characteristics. The standard deviation provides a measure of the variation within each crop, reflecting the degree of heterogeneity or similarity in the spectral properties of the crop pixels. The given PCA analysis, including the *NDVI* band, suggests that the analysis considered the spectral information related to vegetation health and density. The statistics provided for each crop, such as the maximum, mean, minimum, and standard deviation of PCA values, indicate the variability of *NDVI* values within each crop.

By examining the statistics of *NDVI* within each crop, we can infer information about the vegetation health and density characteristics specific to that crop. For example, a higher maximum *NDVI* value suggests dense and healthy vegetation areas. In contrast, a lower mean or standard deviation of *NDVI* values may indicate less variability in vegetation health within the crop area. It is important to note that *NDVI* alone cannot expose crop yield potential [29]. Other factors, such as soil conditions, weather, management practices, and pest/disease pressures, influence crop productivity. However, *NDVI* is a valuable tool for monitoring vegetation health and can be used to indicate crop performance in conjunction with other agronomic data.

4. Conclusions

The main findings of the study can be summarized as follows:

A. The principal component analysis (PCA) revealed strong correlations between specific spectral bands and each crop's principal components (*PC1* and *PC2*). These correlations indicate the importance of specific bands in capturing the variability and characteristics of the crops.
B. Each crop showed distinct correlations between the spectral bands and the principal components. These correlations provide insights into each crop's unique spectral signatures and vegetation characteristics, such as greenness, near-infrared reflectance, and other spectral properties.
C. The equations derived from the PCA analysis provide a mathematical relationship between the spectral bands and the principal components for each crop. These equations can be used to estimate the values of the principal compo- nents based on spectral information, allowing for a better understanding of the crop's characteristics and variability.
D. The analysis of PCA values for each crop revealed variations in the principal components' maximum, mean, min- imum, and standard deviation. These variations indicate differences in the spectral response and variability of the crops, which can be related to vegetation health, density, and productivity.

The implications of these findings are:

1. The study highlights the importance of spectral bands and their correlations with principal components in under- standing the characteristics and variability of different crops. This information can be used to develop crop-specific remote sensing models and monitoring techniques for accurate crop assessment and management.
2. The derived equations provide a means to estimate the principal components based on spectral information. This can be useful for crop monitoring and assessment, allowing for a more comprehensive understanding of crop growth, health, and productivity.
3. The variations in PCA values among crops suggest that each crop has unique spectral signatures and responses. This information can differentiate between crops, monitor their growth stages, identify stress conditions, and assess crop yield potential.
4. The study underscores the value of remote sensing and spectral analysis in crop monitoring and precision agriculture. By integrating spectral information with other agronomic data, such as soil conditions and weather, more informed decisions can be made regarding crop management practices, resource allocation, and yield optimization. Overall, the findings of this study contribute to understanding crop characteristics, variability, and monitoring using re- mote sensing data. They have implications for improving crop management practices, optimizing resource allocation, and enhancing crop productivity in agriculture.

Acknowledgements
This research has been supported by Project BR10865102, "Development of technologies for remote sensing of the earth (RSE) to improve agricultural management," funded by the Ministry of Agriculture of the Republic of Kazakhstan

References

[1] Martos, V, Ahmad, A, Cartujo, P. and Ordoñez, J., (2021). Ensuring Agricultural Sustainability through Remote Sensing in the Era of Agriculture 5.0. *Applied Sciences*, Vol. 11(13). https://doi.org/10.3390/app11135911.

[2] Virnodkar, S. S., Pachghare, V. K., Patil, V. C. and Jha, S. K., (2020). Remote Sensing and Machine Learning for Crop Water Stress Determination in Various Crops: A Critical Review. *Precision Agriculture*, Vol. 21, 1121 - 1155. https://doi.org/10.1007/s11119-020-097 11-9.

[3] Roslim, M. H. M., Juraimi, A. S., Che'Ya, N. N., Sulaiman, N., Manaf, M. N. H. A., Ramli, Z. and Motmainna, M., (2021). Using Remote Sensing and an Unmanned Aerial System for Weed Management in Agricultural Crops: A Review. *Agronomy*, Vol. 11(9). https://doi.org/ 10.3390/agronomy11091809.

[4] Yan, T., Xu, W., Lin, J., Duan, L., Gao, P., Zhang, C. and Lv, X., (2021). Combining Multi-Dimensional Convolutional Neural Network (CNN) With Visualization Method for Detection of Aphis gossypii Glover Infection in Cotton Leaves Using Hyperspectral Imaging. *Front Plant Sci.*, Vol. 15(12). https://doi.org/10.3389/fpls.2021.6045 10.

[5] Zahir, A. D. M., Omar, A. F., Jamlos, M. F., Azmi, M. A. M. and Muncan, J., (2022). A Review of Visible and Near-Infrared (VIS-NIR) Spectroscopy Application in Plant Stress Detection. *Sensors and Actuators A: Physical*, Vol. 338. https://doi.org/10.1016/j.sna.2022. 113468.

[6] Huang, S., Tang, L., Hupy, J. P., Wang, Y. and Shao, G., (2021). A Commentary Review on the Use of Normalized Difference Vegetation Index (NDVI) in the Era of Popular Remote Sensing. *Journal of Forestry Research*, Vol. 32(1). 1– 6. https://doi.org/10.1016/j.sna.2022. 113468.

[7] Zhai, Y., Roy, D. P., Martins, V. S., Zhang, H. K., Yan, L. and Li, Z., (2022). Conterminous United States Landsat-8 Top of Atmosphere and Surface Reflectance Tasseled Cap Transformation Coefficients. *Remote Sensing of Environment*, Vol. 274. https://doi.org/ 10.1016/j.rse.2022.112992.

[8] Sharaf El Din, E., (2021). Enhancing the Accuracy of Retrieving Quantities of Turbidity and Total Suspended Solids Using Landsat- 8-Based-Principal Component Analysis Technique. *Journal of Spatial Science*, Vol. 66(3). 493–512.

[9] Jia, W., Sun, M., Lian, J. and Hou, S., (2022). Feature Dimensionality Reduction: A Review. *Complex & Intelligent Systems*, Vol. 8(3). 2663–2693. https://doi.org/10.1007/s40747-02 1-00637-x.

[10] Skakun, S., Kalecinski, N. I., Brown, M. G. L., Johnson, D. M., Vermote, E. F., Roger, J. C. and Franch, B., (2021). Assessing within-Field Corn and Soybean Yield Variability from WorldView-3, Planet, Sentinel-2, and Landsat 8 Satellite Imagery. *Remote Sens.*, Vol. 2021, 13(5). https://doi.org/10.3390/rs13050872.

[11] Gao, F. and Zhang, X., (2021). Mapping Crop Phenology in Near Real-Time Using Satellite Remote Sensing: Challenges and Opportunities. Journal of Remote Sensing, Vol. 2021(2),1-14.

[12] Gholizadeh, A. and Kopacˇková, V., (2019). Detecting Vegetation Stress as a Soil Contamination Proxy: A Review of Optical Proximal and Remote Sensing Techniques. *International Journal of Environmental Science and Technology*, Vol. 16, 2511–2524. https://doi.org/10.34133/2021/8379391.

[13] da Silva, R. L., Starliper, N., Bhosale, D. K., Taggart, M., Ranganath, R., Sarje, T., Daniele, M., Bozkurt, A., Rufty, T. and Lobaton, E., (2020). Feasibility Study of Water Stress Detection in Plants Using a High-throughput Low-Cost System. *2020 IEEE SENSORS*, 1–4. https://doi.org/10.1109/SENSORS47125.2020 .9278711.

[14] Farber, C., Mahnke, M., Sanchez, L. and Kurouski, D., (2019). Advanced Spectroscopic Techniques for Plant Disease Diagnostics: A Review. *TrAC Trends in Analytical Chemistry*, Vol. 118, 43–49. https://doi.org/10.1016/j. trac.2019.05.022.

[15] Khanal, S., KC, K., Fulton, J. P., Shearer, S. and Ozkan, E., (2020). Remote Sensing in Agriculture—Accomplishments, Limitations, and Opportunities. *Remote Sensing*, Vol. 12(22). https://doi.org/10.3390/rs12223783.

[16] Tamiminia, H., Salehi, B., Mahdianpari, M., Quackenbush, L., Adeli, S. and Brisco, B., (2020). Google Earth Engine for Geo- Big Data Applications: A Meta-Analysis and Systematic Review. *ISPRS Journal of Photogrammetry and Remote Sensing*, Vol. 164, 152–170. https://doi.org/10.1016/j.isprsjprs.2020.04.001

[17] Uuemaa, E., Ahi, S., Montibeller, B., Muru, M, Kmoch, A., (2020). Vertical Accuracy of Freely Available Global Digital Elevation Models (ASTER, AW3D30, MERIT, TanDEM-X, SRTM, and NASADEM). *Remote Sensing*. Vol. 12(21). https://doi.org/10.3390/rs12213482.

[18] Zhang, Y., Schaap, M. G. and Wei, Z., (2020). Development of Hierarchical Ensemble Model and Estimates of Soil Water Retention with Global Coverage. *Geophysical Research Letters*, Vol. 47(15). https://doi.org/10.1029/2020GL088819.

[19] Li, R., Fang, P., Xu, W., Wang, L., Ou, G., Zhang, W. and Huang, X., (2022). Classifying Forest Types Over a Mountainous Area in Southwest China with Landsat Data Composites and Multiple Environmental Factors. *Forests*, Vol. 13(1). https://doi.org/10.3390/f13010135.

[20] Mancino, G., Ferrara, A., Padula, A. and Nolè, A., (2020). Cross-comparison between Landsat 8 (oli) and Landsat 7 (etm+) Derived Vegetation Indices in a Mediterranean Environment. *Remote Sensing*, Vol. 12(2). https://doi.org/10.3390/rs12020291.

[21] Maity, S., Das, S., Pattanayak, J. M., Bera, B. and Shit, P. K., (2022). Assessment of Ecological Environment Quality in Kolkata Urban Agglomeration, India. *Urban Ecosyst.*, Vol. 25, 1137–1154. https://doi.org/10.1007/s11252-022-01220-z.

[22] Arora, R., Cotter, A., Livescu, K. and Srebro, N., (2012). Stochastic Optimization for PCA and PLS. *2012 50th Annual Allerton Conference on Communication, Control, and Computing (Allerton), Monticello, IL, USA, 2012*, 861-868. https://doi.org/10.1109/Allerton.2012.6483308.

[23] Sadenova, M. A., Beisekenov, N. A., Varbanov, P. S., Kulenova, N. A, Abitaev, F. and Kamenev, Y., (2022). Digitalization of Crop Production for Transition to Climate-Optimized Agriculture Using Spring Wheat in East Kazakhstan as An Example. *Chemical Engineering Transactions*, Vol. 96, 415–420. https://doi.org/10.3303/CET2296070.

[24] Adiban, R., Pour, A. H. and Parchami Araghi, F., (2022). Predicting Barley Harvest Time in Dryland Conditions Using Satellite Images. *Yuzuncu Yıl University Journal of Agricultural Sciences*, Vol. 31(3) 655–662. https://doi.org/10.29133/yyutbd.909711.

[25] Xie, C., Yang, C., Hummel Jr, A., Johnson, G. A. and Izuno, F. T., (2018). Spectral Reflectance Response to Nitrogen Fertilization in Field Grown Corn. *International Journal of Agricultural and Biological Engineering*, Vol. 11(4).118– 126.

[26] Degtyareva, O., Muratova, N., Salnikov, V. and Thiel, M., (2019). Monitoring of the Irrigated Rice Production Dynamic in the Kazalinsk Region, Kazakhstan, from 1984-2017. *Central Asian Journal of Water Research*, Vol. 5(2). 20– 43. https://doi.org/10.29258/CAJWR/2019-R1.v5-2/20-43.eng.

[27] Sadenova, M. A., Beisekenov, N. A. and Varbanov, P. S., (2022). Forecasting Crop Yields Based on Earth Remote Sensing Methods. *Chemical Engineering Transactions*, Vol. 92, 691–696. https://www.cetjournal.it/cet/22/92/116.pdf.

[28] Kerimkhulle, S., Kerimkulov, Z., Aitkozha, Z., Saliyeva, A., Taberkhan, R. and Adalbek, A., (2022). The Estimate One-Two-Sided Confidence Intervals for Mean of Spectral Reflectance of the Vegetation. *Journal of Physics: Conference Series*, Vol. 2388, https://doi.org/10.1088/1742-6596/2388/1/012160.

[29] Johnson, D. M., Rosales, A., Mueller, R., Reynolds, C., Frantz, R., Anyamba, A., Pak, E. and Tucker, C., (2021). USA Crop Yield Estimation with MODIS NDVI: Are Remotely Sensed Models Better than Simple Trend Analyses?. *Remote Sensing*, Vol. 13(21). https://doi.org/10.3390/rs13214227.